JOURNAL OF GEOPHYSICAL RESEARCH, VOL. 115, C04011, doi:10.1029/2009JC005576, 2010

Observations of increased wind-driven coastal upwelling off central California

M. García-Reyes[1] and J. Largier[1]

Received 19 June 2009; revised 30 October 2009; accepted 11 November 2009; published 7 April 2010.

[1] Alongshore wind speed and sea surface temperature (SST) from coastal National Data Buoy Center buoys are used to study the variability of wind-driven coastal upwelling from 1982 to 2008. A long-term increase in upwelling is observed in central California (35°N–39°N) with stronger upwelling-favorable winds, colder water, and more frequent occurrences of upwelling days during the upwelling season (March–July). Further, a longer upwelling season is observed in the same region, starting earlier in the spring and persisting later in the fall. These interannual changes in upwelling strength and seasonal duration are investigated in this study. Changes in alongshore wind (forcing of upwelling) are poorly correlated with the El Niño–Southern Oscillation or the Pacific Decadal Oscillation, but the Northern Oscillation and the North Pacific Gyre Oscillation correlate with the geostrophic upwelling-favorable winds in the region. However, changes in SST (an upwelling response) are correlated with both changes in wind (upwelling forcing) and the climate indices. Although this short record cannot differentiate between multidecadal cycles and persistent trends, this data-based result does corroborate model-based projections of increased upwelling in this region due to global climate change. This increase in upwelling is understood to be a response to the strengthening of large-scale pressure gradient fields partially due to global-scale climate change. Farther north and farther south in California, other processes also have a significant influence on coastal conditions, such that the tendency for increased upwelling is not evident in the same way.

Citation: García-Reyes, M., and J. Largier (2010), Observations of increased wind-driven coastal upwelling off central California, *J. Geophys. Res.*, *115*, C04011, doi:10.1029/2009JC005576.

1. Introduction

[2] Coastal upwelling regions are among the most productive areas in the world as alongshore winds drive the upwelling of cold water full of nutrients from depth to the sea surface, enhancing phytoplankton growth. Alongshore winds are due to the large-scale gradient in atmospheric pressure across the coastline, between a high-pressure system over the ocean and a thermal low-pressure system over the landmass. The large scale of these pressure systems makes them sensitive to climate variability; in particular, one may expect to see trends in the strength of these winds and the resultant coastal upwelling process due to climate change. Given the ecological and economic importance of upwelling regions, the question of how the coastal upwelling process is influenced, in strength and timing, by variable climate conditions has received considerable attention. Here we focus attention on direct observations of upwelling winds and sea temperatures over the shelf, i.e., at the scale of the coastal upwelling process.

[3] Annual oceanographic, meteorological, and biological conditions in coastal regions change on different time scales [*Fiedler*, 2002]. In the California Current System, large variability is observed in correlation with the El Niño–Southern Oscillation (ENSO), the Northern Oscillation (NO) [*Schwing et al.*, 2002], the Pacific Decadal Oscillation (PDO) [*Fiedler*, 2002; *Mestas-Nuñez and Miller*, 2006], and the North Pacific Gyre Oscillation (NPGO) [*Di Lorenzo et al.*, 2008]. The positive phases of ENSO, El Niño events, cause anomalous warm water temperatures in the coastal waters [*McGowan et al.*, 1998; *Lluch-Cota et al.*, 2001; *Di Lorenzo et al.*, 2005; *Mestas-Nuñez and Miller*, 2006], resulting in decreased primary productivity [*Chavez et al.*, 2002; *Kahru and Mitchell*, 2002; *Chavez et al.*, 2003], with reversed effects during the negative phases (i.e., La Niña events). The NO, with similar variability and character as ENSO, is correlated with changes in the North Pacific High and is therefore correlated with changes in upwelling-favorable winds along the northeastern Pacific [*Schwing et al.*, 2002]. The interannual variability of ENSO has a time scale of 5–6 years [*Ghil and Vautard*, 1991]; however, this variability is modulated by the PDO [*Mantua and Hare*,

[1]Bodega Marine Laboratory, University of California, Davis, Bodega Bay, California, USA.

0148-0227/10/2009JC005576

2002; *Mestas-Nuñez and Miller*, 2006], while the NO has a decadal variability of around 14 years [*Schwing et al.*, 2002]. The PDO is defined as the first empirical orthogonal function (EOF) of the sea surface temperature (SST) field, and the NPGO is defined as the second EOF of the sea surface height field in the North Pacific [*Mantua and Hare*, 2002; *Di Lorenzo et al.*, 2008]. The PDO signal along the California coast is similar to ENSO for SST [*Mantua and Hare*, 2002; *Peterson and Schwing*, 2003; *Mestas-Nuñez and Miller*, 2006], with PDO influence being stronger north of 38°N [*Lluch-Cota et al.*, 2001; *Di Lorenzo et al.*, 2008] and ENSO influence being stronger off southern California [*Lluch-Cota et al.*, 2001; *Mestas-Nuñez and Miller*, 2006]. The NO influence on SST is uniform along California [*Schwing et al.*, 2002]. NPGO is correlated with salinity, nutrient, and chlorophyll contents, which are driven by coastal upwelling, particularly south of 38°N [*Di Lorenzo et al.*, 2008]. The ecosystem exhibits large and drastic changes with the PDO and NPGO phases [see, e.g., *Chavez et al.*, 2002; *Fiedler*, 2002; *Peterson and Schwing*, 2003; *Kahru et al.*, 2009]. The mechanism behind these decadal oscillations is unknown [*Mantua and Hare*, 2002], and it is not clear if they are independent of NO or ENSO (for a review of the proposed mechanism see *Mestas-Nuñez and Miller* [2006]).

[4] Observed and projected increases in global temperature (i.e., global warming) raise the question about how the upwelling process and, in consequence, the coastal ocean ecosystem, will change. In 1990, *Bakun* [1990, p. 198] proposed that global greenhouse warming

> should lead to intensification of the continental thermal lows adjacent to upwelling regions. This intensification would be reflected in increased onshore-offshore atmospheric pressure gradients, enhanced alongshore winds, and accelerated coastal upwelling circulation

that would result in cooling of the ocean surface. A number of studies on different upwelling regions have investigated this trend using data and numerical models.

[5] Numerical simulations for the California Current System show that increased CO_2 concentration in the atmosphere leads to intensification of the upwelling-favorable winds [*Snyder et al.*, 2003; *Di Lorenzo et al.*, 2005; *Auad et al.*, 2006; *Di Lorenzo et al.*, 2008]. However, surface heating is expected to lead to warmer surface water, deeper thermocline, and higher stratification, which counteract the effect of stronger upwelling winds. The net result would depend on the relative magnitude of these two effects: wind forcing and surface heating. In a model study, *Di Lorenzo et al.* [2005] found that for the 1949–2000 period, the effect of the increase in upwelling winds in southern California was smaller than the surface warming effect, resulting in net warming conditions. However, in a projection done by *Auad et al.* [2006], given larger CO_2 concentrations in the future, the increase in upwelling winds overcomes the increase in thermal stratification so that more upwelling is expected, in particular for central California during April. Another projection done by *Snyder et al.* [2003] found increased upwelling conditions in August–September off San Francisco Bay and to the north. Further, a numerical simulation done by *Di Lorenzo et al.* [2008] found that the amplitude of NPGO (which is correlated to coastal upwelling) increases under a global warming scenario.

[6] The question of long-term changes in upwelling can also be investigated through an analysis of available data. However, time series data are limited in duration, quality, and/or spatial extent. The available long-term, spatially extensive time series are synthetic data sets (e.g., Comprehensive Ocean-Atmosphere Data Set (COADS) and National Centers for Environmental Prediction (NCEP) reanalysis) that incorporate measurements with different spatial and temporal representation and with a spatial resolution that is too coarse to resolve conditions at the scale of coastal upwelling (scales of order 10 km). Nevertheless, studies using these data find increased upwelling along the California coast over recent decades. *Bakun* [1990] reports an increase in the upwelling index (calculated from atmospheric pressure records) while *Mendelssohn and Schwing* [2002] report trends of stronger wind and decreased SST from an analysis of April–September COADS data for 1940–1990. However, this increased upwelling takes place only in central California (32°N–40°N), with a decrease in upwelling-favorable winds observed north of 40°N and an increase in SST observed south of 32°N.

[7] Similar trends are found in other upwelling systems. *Bakun* [1990] and *Mendelssohn and Schwing* [2002] found increased upwelling in the Peru-Chile Current System (PCCS). Furthermore, *Mendelssohn and Schwing* [2002] found regions in the PCCS with different interannual and interdecadal fluctuations in upwelling intensity, similar to California. Comparing these two systems, *Mendelssohn and Schwing* [2002] suggested that the state of the upwelling regions is influenced by global scale forcing. Similarly, in the Canary Current System, *Santos et al.* [2005] found different upwelling fluctuations in different zones. In the southern Canary Current, off northwest Africa, *Bakun* [1990] and *McGregor et al.* [2007] found increased upwelling and decreased temperatures since 1950. However, while *Bakun* [1990] found increased upwelling off the Iberian Peninsula in the northern Canary Current from 1950 to 1980, other studies found decreased upwelling [*Lemos and Pires*, 2004; *Álvarez-Salgado et al.*, 2008] and a smaller number of upwelling days [*Mason et al.*, 2005; *Álvarez-Salgado et al.*, 2008].

[8] These prior studies have focused on spatial scales larger than that of the coastal upwelling process, which typically occurs within 10 km of the shore in intense and localized upwelling zones [*Capet et al.*, 2004; *Kirincich et al.*, 2005] or within a few multiples of 10 km where wind curl patterns are important [*Dever et al.*, 2006]. Cold water and enhanced biological production may extend farther offshore in plumes of upwelled water advected offshore, influencing the California Current System [*Lynn et al.*, 2003]. This prior focus on larger scales was necessitated by the coarse spatial data and coarse wind forcing for numerical models, although numerical simulations are accurate in predicting the upwelling conditions only when the nearshore wind profile is well represented [*Capet et al.*, 2004]. However, some prior studies have indicated that interannual variability in coastal conditions is larger than that for offshore waters in upwelling systems [*McGowan et al.*, 1998; *Lluch-Cota et al.*, 2001; *Mestas-Nuñez and Miller*, 2006]. So, while COADS and the Bakun upwelling index illuminate changes at the scale of the California Current, our interest is to investigate interannual changes in the coastal upwelling

Table 1. NDBC Buoy Information[a]

Coastal							
Buoy	Latitude (°N)	Longitude (°W)	Year[b]	Orientation[c]	Axis[d]	Missing Data (%)	Gap (years)[e]
N27	41.85	124.38	1983	345	338	29	1.4
N22	40.78	124.54	1982	357	353	15	0.8
N14	39.22	123.97	1981	333	328	15	0.9
N13	38.23	123.32	1981	310	313	13	1.1
N26	37.75	122.82	1982	310	315	16	0.8
N12	37.36	122.88	1980	333	329	29	1.7
N42	36.75	122.42	1986	330	324	36	2.5
N28	35.74	121.88	1983	325	321	29	1.1
N11	34.87	120.86	1980	327	322	24	1.8
N23	34.71	120.97	1982	327	322	14	0.9
N25	33.74	119.06	1982	290	289	6	0.4

[a]Buoy labels are abbreviated (e.g., NDBC46027 is abbreviated to N27).
[b]Initial year of data (all data end in 2008).
[c]Coastal orientation angle from *Dorman and Winant* [1995] (clockwise degrees from true north).
[d]Principal axis of the wind at the buoy location.
[e]Extent of the largest gap in the daily time series.

process. In this work, we use 27 years of hourly data on winds and SST over the shelf, which are available from buoys deployed by the National Data Buoy Center (NDBC). There are also some long-term records from shore stations, but they are confounded by local nearshore effects (e.g., in regions sheltered from upwelling), and thus we do not use these data here. We use alongshore wind speed as an index of upwelling forcing and SST as an index of upwelling response. Although changes in SST include the effects of upwelling and surface heating, the latter effect is considered secondary in active upwelling zones as the NDBC buoys over the shelf monitor waters that are recently upwelled. Here we report interannual trends in these wind and temperature data as the most direct observation of trends in the coastal upwelling process along the Californian coast.

2. Data and Methodology

[9] Twenty-seven years (1982–2008) of hourly wind and SST data from NDBC buoys (http://www.ndbc.noaa.gov) over the California shelf are used to study coastal upwelling conditions at different latitudes. The position and features of each buoy are described by *Dorman and Winant* [1995] and are summarized in Table 1 and Figure 1.

[10] The NDBC data used are wind speed (m s^{-1}), wind direction (degrees from true north), and SST (°C), in hourly records that are averaged into daily values. As coastal upwelling is forced by the alongshore component of the wind, the orientation of the shore and bathymetry must be determined. Off California, the principal axis of wind variability and the coastal orientation are similar at each buoy location (difference <7°) as strong coastal orography forces winds to blow parallel to the coast [*Dorman and Winant*, 1995]. Given that the coastal orientation measurement depends on the scale used, we use the wind speed along the principal axis as the best way to define the alongshore wind component. Using conventional right-handed coordinates, negative values of this alongshore wind speed (AWS) are in the equatorward direction and are upwelling favorable.

[11] Gaps in each buoy time series were filled using a linear regression with data from the nearest buoy. The correlation coefficient between each pair of neighboring buoys is larger than 0.75 for SST and larger than 0.9 for AWS (except for buoy N25 in the Southern California Bight). When the gaps cannot be filled with the original data from the nearest buoy, gap-filled data from that buoy were used. Only data from 1982 to 2008 are used in the analysis; longer time series were cut and the shorter ones filled, so all time series have the same length for this analysis.

[12] The climatology for each buoy is calculated by averaging the 27 values available for each day of the year (one value from each year of data). Then, the resulting yearlong time series is filtered using a low-pass filter with a cutoff period of 29 days (Figures 2a and 2b). This climatology is used to identify the typical upwelling season for each location and to calculate daily anomalies. Monthly values are calculated by averaging daily values, and monthly anomalies are calculated by averaging the daily anomalies.

[13] The timing and length of the upwelling season vary with latitude, being shorter for northern California and year-round for southern California. However, from March to July, upwelling conditions are present at most locations in most years. Therefore, we used this period as a standard upwelling season to compare trends in upwelling intensity across sites. The average of the daily anomalies during this period is used to characterize the upwelling season (Figures 2c and 2d). For other analyses, data from the entire year are analyzed.

[14] To estimate the total annual amount of coastal upwelling at each location, the number of days with upwelling conditions is counted. The Ekman transport response to upwelling winds is lagged by less than a day [*Lentz*, 1992];

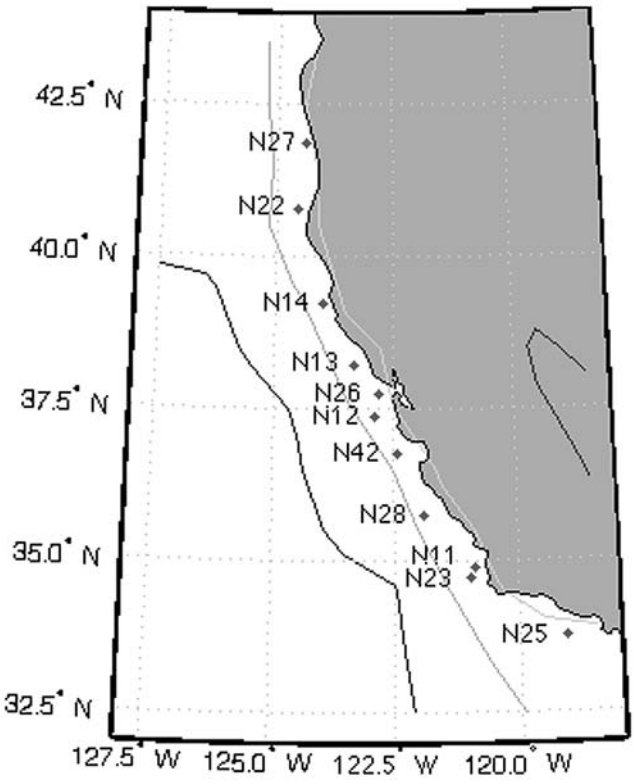

Figure 1. NDBC buoy locations.

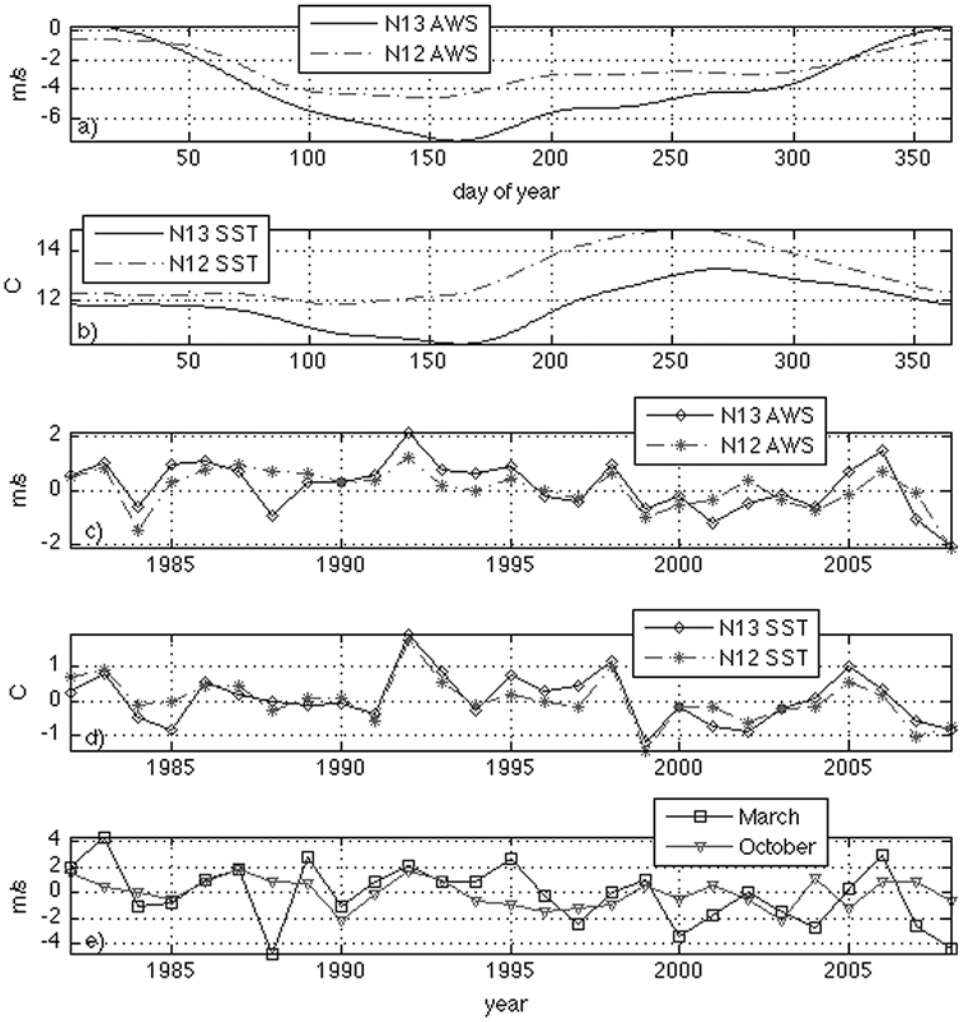

Figure 2. Time series for buoys N13 (Bodega Bay) and N12 (Half Moon Bay). (a) Climatology for AWS, (b) climatology for SST, (c) AWS upwelling season means, (d) SST upwelling season means, and (e) time series of March and October AWS monthly anomalies for buoy N13.

however, it takes a longer period for cold, nutrient-rich water to reach the surface and to be available for primary production. Both *Botsford et al.* [2006] and *Dugdale et al.* [2006] indicate that 3 days of wind forcing are required for the event to be ecologically important in this way. Therefore, we class a day as an upwelling day only when the wind has been over a threshold for at least 3 days. We also count the number of days that SST is below a threshold; we count this simply since SST is a response variable and low values indicate that upwelling has occurred and cold, high-nutrient water is already at the surface at the midshelf buoy site. Finally, we count the number of days that both conditions are met. AWS and SST threshold values that separate nonupwelling and upwelling conditions are chosen for each buoy on the basis of the buoy climatology.

[15] During the spring there is a marked transition to upwelling conditions of strong equatorward winds and colder water off northern California and Oregon, but this spring transition is less marked off central California [*Dorman and Winant*, 1995]. While the spring transition refers to a period more than a specific day [*Lentz*, 1987; *Lynn et al.*, 2003], in order to calculate its change with time in this study, the spring transition is identified as the first time concurrent wind, and temperature upwelling conditions are observed (as described above). A short and isolated wind event before the upwelling season (e.g., a single event in 2 weeks) is not taken into account as such isolated events occur commonly during the winter and do not shift the ocean conditions to an upwelling state [*Lentz*, 1987]. Similarly, the last day with upwelling conditions is considered the end of the upwelling season.

[16] The coastal upwelling index (UI) (units of $m^3\ s^{-1}\ (100\ m)^{-1}$) is a commonly used index of upwelling strength provided by the Pacific Fisheries Environmental Laboratory at NOAA. It is calculated from geostrophic winds which are derived from pressure fields over the northeast Pacific [*Bakun*, 1973]. Monthly values of UI are available from 1967 for the California coast with a resolution of 1° × 1°, calculated specifically for the coastal orientation at the given latitude (http://www.pfeg.noaa.gov/products/las/docs/global_upwell.html). UI monthly anomalies are obtained from a monthly climatology calculated for the same period as the wind.

[17] In addition, the following time series of annual indices were constructed as a basis for analysis of interannual

Table 2. AWS, SST, and UI Upwelling Season Trends for 1982–2008[a]

Buoy	AWS ($m\ s^{-1}\ yr^{-1}$)	SST ($°C\ yr^{-1}$)	UI ($m^3\ s^{-1}\ (100\ m)^{-1}\ yr^{-1}$)	AWS Days[b] ($d\ yr^{-1}$)	AWS and SST Days[b] ($d\ yr^{-1}$)	Spring[c] ($d\ yr^{-1}$)	Fall[c] ($d\ yr^{-1}$)
N27	−0.005	0.000	**3.82**	−0.279	−0.037	−0.827	1.368
N22	−0.021	−0.001	**4.89**	**0.606**	0.195	−0.822	1.906
N14	−0.014	−0.028	**2.67**	−0.271	0.192	−0.384	−1.542
N13	**−0.050**	−0.017	**2.13**	0.535	0.432	**−1.114**	−0.558
N26	**−0.059**	**−0.032**	**1.10**	**1.371**	**0.680**	0.206	**3.421**
N12	**−0.043**	**−0.034**	**1.10**	**0.794**	**0.326**	−0.992	0.721
N42	**−0.045**	−0.021	**1.12**	**1.277**	**0.419**	−0.386	0.550
N28	**−0.037**	−0.025	**1.34**	**1.131**	**0.766**	−1.071	0.781
N11	−0.003	−0.041	**1.09**	0.185	**0.484**	−0.334	0.379
N23	0.037	**−0.043**	**1.09**	**−1.708**	0.367	1.551	−0.696
N25	0.012	**−0.003**	−0.51	**−0.869**	**0.230**	0.294	−0.603

[a]Bold values indicate a level of significance at $p < 0.1$.
[b]Trends for the number of upwelling days.
[c]Trends for the spring and fall transitions.

trends in upwelling: (1) upwelling season means for AWS, SST, and UI anomalies with one value per year, averaged from March to July (UI data are only considered from 1982 to 2008 to match the period of the NDBC data) (Figures 2c and 2d); (2) number of upwelling days per year defined by AWS upwelling days and by both AWS and SST conditions; (3) spring transition, the day when the first non-isolated upwelling event starts (one value per year); (4) fall transition, the last day with upwelling conditions (one value per year); and (5) maximum and minimum values of AWS and SST for each year, defined as the 90th and 10th deciles of the upwelling-season daily data to track the intensity of upwelling.

[18] Trends in these indices were calculated using ordinary linear regressions with a significance level of $p = 0.1$. In addition, a delete-1 jackknife method [*Emery and Thomson*, 2004] was applied to each time series trend to assess the error of outlier years in the calculation of the trend. Standard errors for the jackknife method were calculated including the effect of autocorrelation.

[19] In addition, time series of climate indices were obtained from the Web sites http://www.esrl.noaa.gov/psd/data/climateindices/list and http://www.o3d.org/npgo. Correlations were calculated between the large-scale multivariate ENSO index and PDO, NO, and NPGO indices (averaged from March to July) and upwelling-season time series for AWS, SST, and UI. The correlation between climate indices and local parameters is best at different lags. However, the correlation at zero lag differs little from that at optimal lag. As our interest is in interannual changes, we use zero lag for all calculations of these correlations.

3. Results

[20] The trends for upwelling season means are shown in Table 2 and Figure 3. Significant increasing trends of

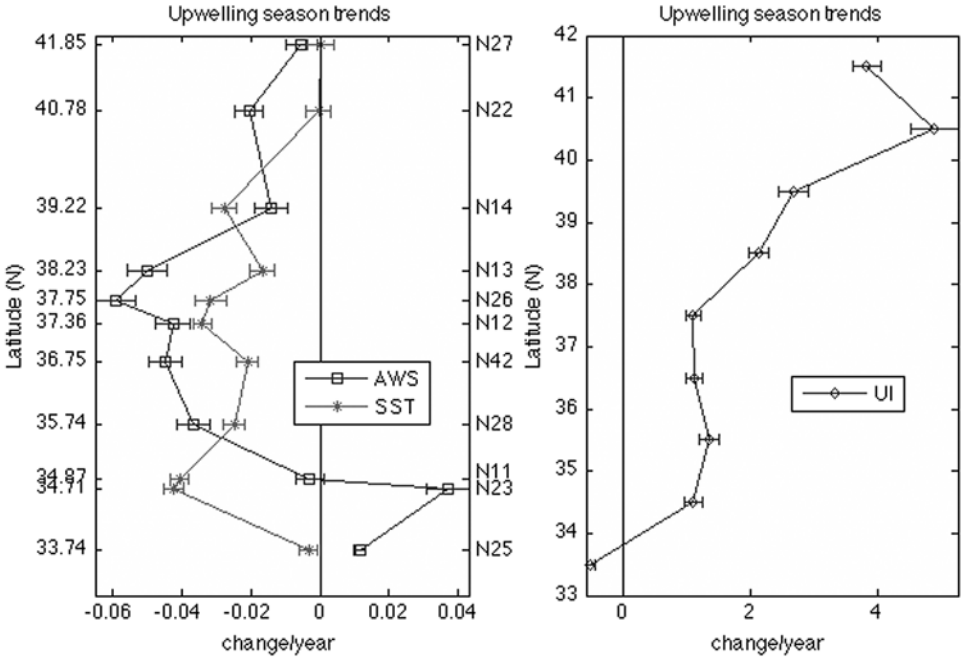

Figure 3. Trends of the upwelling season means (and standard error) for all locations. (left) AWS ($m\ s^{-1}\ yr^{-1}$) and SST ($°C\ yr^{-1}$). (right) UI ($m^3\ s^{-1}\ (100\ m)^{-1}\ yr^{-1}$).

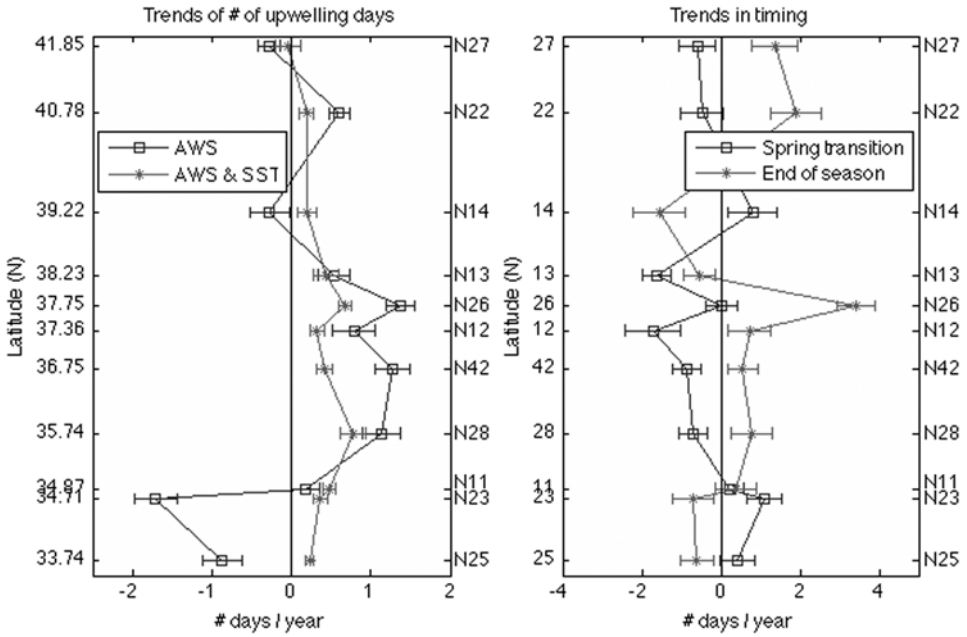

Figure 4. (left) Trends of number of days with upwelling-favorable winds (squares) and trends of number of days with both strong winds and cold SST (stars). (right) Trends of the spring transition (squares) and end of season (stars) time series. Trends given in d yr^{-1}.

upwelling winds (more negative AWS) are observed for central California, between 35°N and 39°N, at buoys N13, N26, N12, N42, and N28, and for UI north of 34.5°N. Decreasing SST trends are more widespread, from Cape Mendocino (40°N) south to Point Conception (34°N); however, more significant trends are observed for buoys N26, N12, N11, and N23.

[21] Three geographical regions are thus evident on the basis of the calculated AWS trends. These regions coincide with the classification of *Dorman and Winant* [1995] based on the characteristics of the upwelling season: (1) northern California, buoys N27, N22, and N14; (2) central California, buoys N13, N26, N12, N42, and N28; and (3) southern California, buoys N11, N23, and N25.

[22] There is a trend toward more upwelling days off central California, most marked by an increase in strong wind days at buoys N26, N12, N42, and N28 but also seen as a milder but more widespread increase in the number of days with upwelling-favorable winds and cold SST along the entire California coast (Table 2 and Figure 4). The trends for spring transition and the end of the season are less significant, as the variability on the dates is large, but there is a tendency for an earlier start and a later end to the upwelling season in the central California region. This lengthening of the upwelling season is consistent with a clear trend of increased upwelling in early and late upwelling season months (March and October) off northern and central California (Figure 2e). Also, a positive trend in the number of upwelling days in March and October is observed in the same region, and also in September, for central California.

[23] Trends in high and low values (90th and 10th decile values, not shown) indicate that the intensity of the strongest upwelling wind events have increased in central California, whereas weaker winds show a trend to being weaker or increasingly poleward. This indicates an increased variability in the winds: stronger upwelling events but relaxation events with weaker or more poleward winds. The variability is also observed in an increased standard deviation of the daily wind data through the years. Lowest-decile SST values are colder for central and southern California, and highest-decile values are also colder off central California. This is consistent with the decrease in mean SST during the upwelling season (Figure 3). SST variability in the upwelling season has changed little.

[24] Correlations between March–July means of climate indices and AWS are best for central California, in particular for NO ($r \approx -0.7$). In the northern region the correlation decreases slightly, but it increases for PDO ($r \approx +0.6$). UI correlates best with NO ($r > +0.6$) around 36.5°N and with NPGO ($r > +0.6$) for central and southern California. SST correlates best with NO ($r < -0.7$) for central California and buoys N14, N11, and N23. SST also correlates with ENSO and PDO ($r > +0.6$) for central California and with PDO ($r > +0.7$) for the northern region. The correlation of NPGO with SST is around −0.6 for central California.

4. Discussion

[25] A clear trend toward stronger upwelling off California is evident in a quarter century of coastal wind and SST data, consistent with Bakun's hypothesis. Enhanced upwelling is observed in central California (35°N–39°N), with stronger upwelling-favorable winds, colder water, and more frequent occurrence of upwelling days. This is the first study of long-term trends in data that are exclusively coastal (i.e., over the shelf) and that can thus be reliably interpreted as a change in the coastal upwelling process. Prior analyses by *Bakun* [1990] and *Mendelssohn and Schwing* [2002] were for an area that extended far off the shelf and better represented the offshore California Current System than the active upwell-

ing process over the shelf. Further, this analysis is of recent data, including the 1998 El Niño, the strong negative PDO event in 1999, and the shift since 1999 to a period of decreased ENSO activity.

[26] The clear trend toward increased upwelling winds in central California is consistent with Bakun's hypothesis [*Bakun*, 1990] as the largest change is expected in regions where upwelling is the dominant process [*Di Lorenzo et al.*, 2005], i.e., central California [*Dorman and Winant*, 1995]. The lengthening of the upwelling season is mainly due to increased upwelling wind in March in the early season and in August–October in the late season, similar to numerical predictions [*Snyder et al.*, 2003; *Auad et al.*, 2006]. The only exception is the Gulf of Farallones, where the upwelling season is clearly extended into the fall but with no change in timing of the spring transition.

[27] The observed decrease in SST is limited to coastal waters over the shelf, where the upwelling process dominates. In contrast, data from the central North Pacific show a warming trend for the same period, explained partially by the PDO and partially by a global secular trend [*Field et al.*, 2006]. Similarly, in nearshore bays, coves, and estuaries other trends may be observed as the effect of long-term changes in surface heating and/or runoff may dominate the observed changes in upwelling. Further, some of the buoy-to-buoy differences within a region are presumably due to local influences, with buoys such as N26 and N12 being partially sheltered from upwelling winds in the Gulf of Farallones and buoys N11 and N23 being in the path of cold upwelled waters streaming south from the central California coast irrespective of local changes in alongshore winds. Although secondary local effects exist, our emphasis here is on regional phenomena, with additional confidence coming from the observation of common trends in independent records obtained at adjacent buoys.

[28] At buoys off northern California (specifically N27 and N22), the changes in upwelling are mixed, which we understand as being due to the role of cold-front wind events during the upwelling season, specifically early in the season [*Dorman and Winant*, 1995]. The UI increases in both central and northern California (34°N–41°N), but it reflects geostrophic winds only and thus underestimates the influence of frontal winds that are more common in the north. Further, this index is averaged over a long distance offshore and fails to reflect the effect of topographic features that enhance upwelling winds (e.g., Cape Mendocino and Point Arena). The trend to increasing UI is largest at these northern locations; however, this increase in the upwelling driver is not reflected in the SST response, suggesting that coastal upwelling is not the dominant process. In addition, at these northern sites SST may be also affected by seasonal cooling in addition to upwelling, in contrast to central California, where the coldest SST is observed in spring and early summer because of upwelling.

[29] In southern California, the decreased upwelling-favorable winds and UI and the cooler SST contrast with the results from *Di Lorenzo et al.* [2005]. However, decreasing SST in Point Conception buoys is presumably related to the advection of upwelled water from central California. Buoy N25 is located well inside the Southern California Bight, shielded from the advection of cold water from central California, and it has a completely different AWS and SST climatology (not shown) and different trends than buoys N11 and N23.

[30] Given that data are only available for 27 years, we cannot identify trends longer than this period and cannot separate a long-term oscillation from a persistent trend. It is interesting to note that the trends in AWS in central California can be partially explained by trends in the NO and NPGO indices. However, this is not to say that this part of the signal is not a persistent trend as the NPGO and NO indices may also be effective indices of persistent trends (although they were developed to highlight fluctuations in atmosphere and ocean conditions). For example, numerical models predict a stronger NPGO in a warming future [*Di Lorenzo et al.*, 2008], consistent with stronger coastal upwelling. Likewise, SST is correlated with ENSO and PDO indices, all perhaps reflecting a common underlying changing climate. However, in this regard, there is an important difference in spatial pattern with the PDO signal being stronger in the north and the ENSO signal being stronger in the south, whereas the observed signal in the SST trend is strongest in central California. Second, the spatial pattern of trends in SST correlates well with the trends in AWS. Finally, it is worth noting that NO and NPGO are indices of North Pacific Ocean conditions, whereas increases in upwelling have been reported from other regions [*Bakun*, 1990; *Mendelssohn and Schwing*, 2002; *Santos et al.*, 2005; *McGregor et al.*, 2007], suggesting a more global phenomenon.

[31] In summary, a clear trend of stronger coastal upwelling is observed in central California from 1982 to 2008, in particular from Monterey Bay to Bodega Bay (35°N–39°N). Although the record is too short to statistically separate the observed trends from the influence of decadal oscillations associated with NO, NPGO, ENSO, and PDO, the localized region where the trends are observed and their correlation with similar trends in the NO and NPGO indices suggest a change in the strength of wind-driven coastal upwelling rather than a change in the conditions of the California Current. The observed wind and SST records are short, but these data along with model predictions suggest that a secular trend in global temperatures may have already led to increased upwelling off central California and perhaps also in other coastal upwelling regions.

[32] **Acknowledgments.** This work is supported in part by the National Science Foundation under award ATM-0619139, Coast-to-Mountain Environmental Transect (COMET) project.

References

Álvarez-Salgado, X. A., U. Labarta, M. J. Fernández-Reiriz, F. G. Figueiras, G. Rosón, S. Piedracoba, R. Filgueira, and J. M. Cabanas (2008), Renewal time and the impact of harmful algal blooms on the extensive mussel raft culture of the Iberian coastal upwelling system (SW Europe), *Harmful Algae*, *7*, 849–855.

Auad, G., A. Miller, and E. Di Lorenzo (2006), Long-term forecast of oceanic conditions off California and their biological implications, *J. Geophys. Res.*, *111*, C09008, doi:10.1029/2005JC003219.

Bakun, A. (1973), Coastal upwelling indices, west coast of North America, 1946–71, *NOAA Tech. Rep. NMFS SSRF-671*, 103 pp.

Bakun, A. (1990), Global climate change and intensification of coastal ocean upwelling, *Science*, *247*, 198–201.

Botsford, L. W., C. A. Lawrence, E. P. Dever, A. Hasting, and J. Largier (2006), Effects of variable winds on biological productivity on continental

shelves in coastal upwelling systems, *Deep Sea Res., Part II*, *53*, 3116–3140, doi:10.1016/j.dsr2.2006.07.011.
Capet, X. J., P. Marchesiello, and J. C. McWilliams (2004), Upwelling response to coastal wind profiles, *Geophys. Res. Lett.*, *31*, L13311, doi:10.1029/2004GL020123.
Chavez, F. P., J. T. Pennington, C. G. Castro, J. P. Ryan, R. P. Michisaki, B. Schlining, P. Walz, K. R. Buck, A. McFadyen, and C. A. Collins (2002), Biological and chemical consequences of the 1997–1998 El Niño in central California waters, *Progr. Oceanogr.*, *54*, 205–232.
Chavez, F. P., J. Ryan, S. E. Lluch-Cota, and M. Ñiquen C. (2003), From anchovies to sardines and back: Multidecadal change in the Pacific Ocean, *Science*, *299*, 217–221, doi:10.1126/science.1075880.
Dever, E. P., C. E. Dorman, and J. L. Largier (2006), Surface boundary-layer variability off northern California, USA, during upwelling, *Deep Sea Res., Part II*, *53*, 2887–2905.
Di Lorenzo, E., A. J. Miller, N. Schneider, and J. C. McWilliams (2005), The warming of the California Current System: Dynamics and ecosystem implications, *J. Phys. Oceanogr.*, *35*, 336–362.
Di Lorenzo, E., et al. (2008), North Pacific Gyre Oscillation links ocean climate and ecosystem change, *Geophys. Res. Lett.*, *35*, L08607, doi:10.1029/2007GL032838.
Dorman, C. E. and C. D. Winant (1995), Buoy observations of the atmosphere along the West Coast of the United States, 1981–1990, *J. Geophys. Res.*, *100*, 16,029–16,044.
Dugdale, R. C., F. P. Wilkerson, V. E. Hogue, and A. Marchi (2006), Nutrient controls on new production in the Bodega Bay, California, coastal upwelling plume, *Deep Sea Res., Part II*, *53*, 3049–3062.
Emery, W. J., and R. E. Thomson (2004), *Data Analysis Methods in Physical Oceanography*, 2nd ed., pp. 294–304, Elsevier, Amsterdam.
Fiedler, P. C. (2002), Environmental change in the eastern tropical Pacific Ocean: Review of ENSO and decadal variability, *Mar. Ecol. Prog. Ser.*, *244*, 265–283.
Field, D., D. Cayan, and F. Chavez (2006), Secular warming in the California Current and North Pacific, *Calif. Coop. Oceanic Fish. Invest. Rep.*, *47*, 92–108.
Ghil, M., and R. Vautard (1991), Interdecadal oscillation and the warming trend in global temperature time series, *Nature*, *350*, 324–327.
Kahru, M. and B. G. Mitchell (2002), Influence of the El Niño–La Niña cycle on satellite-derived primary production in the California Current, *Geophys. Res. Lett.*, *29*(17), 1846, doi:10.1029/2002GL014963.
Kahru, M., R. Kudela, M. Manzano-Sarabia, and B. G. Mitchell (2009), Trends in primary production in the California Current detected with satellite data, *J. Geophys. Res.*, *114*, C02004, doi:10.1029/2008JC004979.
Kirincich, A. R., J. A. Barth, B. A. Grantham, B. A. Menge, and J. Lubchenco (2005), Wind-driven inner-shelf circulation off central Oregon during summer, *J. Geophys. Res.*, *110*, C10S03, doi:10.1029/2004JC002611.
Lemos, R. T., and H. O. Pires (2004), The upwelling regime off the west Portuguese coast, 1941–2000, *Int. J. Climatol.*, *24*, 511–524, doi:10.1002/joc.1009.
Lentz, S. J. (1987), A description of the 1981 and 1982 spring transitions over the northern California shelf, *J. Geophys. Res.*, *92*, 1545–1567.
Lentz, S. J. (1992), The surface boundary layer in coastal upwelling regions, *J. Phys. Oceanogr.*, *22*, 1517–1539.
Lluch-Cota, D. B., W. S. Wooster, and S. R. Hare (2001), Sea surface temperature variability in coastal areas of the northeastern Pacific related to the El Niño–Southern Oscillation and the Pacific Decadal Oscillation, *Geophys. Res. Lett.*, *28*, 2029–2032.
Lynn, R. J., S. J. Bograd, T. K. Chereskin, and A. Huyer (2003), Seasonal renewal of the California Current: The spring transition off California, *J. Geophys. Res.*, *108*(C8), 3279, doi:10.1029/2003JC001787.
Mantua, N. J., and S. R. Hare (2002), The Pacific Decadal Oscillation, *J. Oceanogr.*, *58*, 35–44.
Mason, E., A. M. P. Santos, and A. J. Peliz (2005), Western Iberian winter wind indices based on significant wind events, *Ocean Sci. Discuss.*, *2*, 105–127.
McGowan, J. A., D. R. Cayan, and L. M. Dorman (1998), Climate-ocean variability and ecosystem response in the northeast Pacific, *Science*, *281*, 210–217.
McGregor, H. V., M. Dima, H. W. Fischer, and S. Mulitza (2007), Rapid 20th-century increase in coastal upwelling off northwest Africa, *Science*, *315*, 637–639, doi:10.1126/science.1134839.
Mendelssohn, R. and F. B. Schwing (2002), Common and uncommon trends in SST and wind stress in California and Peru-Chile current systems, *Progr. Oceanogr.*, *53*, 141–162.
Mestas-Nuñez, A. M., and A. J. Miller (2006), Interdecadal variability and climate change in the eastern tropical Pacific: A review, *Progr. Oceanogr.*, *69*, 267–284, doi:10.1016/j.pocean.2006.03.011.
Peterson, W. T., and F. B. Schwing (2003), A new climate regime in northeast Pacific ecosystems, *Geophys. Res. Lett.*, *30*(17), 1896, doi:10.1029/2003GL017528.
Santos, A. M. P., A. S. Kazmin, and A. Peliz (2005), Decadal changes in the Canary upwelling system as revealed by satellite observations: Their impact on productivity, *J. Mar. Res.*, *63*, 359–379.
Schwing, F. B., T. Murphree, and P. M. Green (2002), The Northern Oscillation Index (NOI): A new climate index for the northeast Pacific, *Progr. Oceanogr.*, *53*, 115–139.
Snyder, M. A., L. C. Sloan, N. S. Diffenbaugh, and J. L. Bell (2003), Future climate change and upwelling in the California Current, *Geophys. Res. Lett.*, *30*(15), 1823, doi:10.1029/2003GL017647.

M. García-Reyes and J. Largier, Bodega Marine Laboratory, University of California, Davis, Bodega Bay, CA 94923, USA. (solgarcia@ucdavis.edu; jlargier@ucdavis.edu)